Guanine tautomerism revealed by UV–UV and IR–UV hole burning spectroscopy

E. Nir
Department of Chemistry, The Hebrew University, Jerusalem 91904, Israel

Ch. Janzen, P. Imhof, and K. Kleinermanns
Institut für Physikalische Chemie und Elektrochemie I, Heinrich Heine Universität Duesseldorf, 40225 Düsseldorf, Germany

M. S. de Vries
Department of Chemistry and Biochemistry, Santa Barbara, California 93106

(Received 17 January 2001; accepted 20 June 2001)

The vibronic spectrum of laser desorbed and jet cooled guanine consists of bands from three different tautomers of guanine as revealed by UV–UV and IR–UV double resonance spectroscopy. 1-methylguanine, in which the Keto–Enol tautomerism is blocked, shows hole burning spectra from the 9H-and 7H-Keto form. A comparison of the vibronic pattern of the different tautomers demonstrates that the vibronic spectrum built on the redmost guanine band at 32 870 cm^{-1} (electronic origin 0) can be traced back to the 9H-Enol tautomer, while the spectra built on the origins at $0+404\,cm^{-1}$ and $0+1044\,cm^{-1}$ stem from the two Keto tautomers. The IR–UV double resonance spectra of the OH-and NH-stretch vibrations of the different tautomers support this assignment. The UV and IR spectra can be partly assigned by comparison with *ab initio* calculated vibrational frequencies and with the help of deuteration experiments. © *2001 American Institute of Physics.* [DOI: 10.1063/1.1391443]

I. INTRODUCTION

The DNA bases have been the subjects of many theoretical and experimental investigations because of their biological importance.[1–4] In the gas phase the intrinsic properties of the bases can be studied without intermolecular interactions at vibrational or even rotational resolution.[5–15] Though small, they are difficult to vaporize without extensive decomposition and guanine in particular cannot be vaporized intact by simple thermal heating. Recently, the vibronic spectrum of laser desorbed, jet cooled guanine was obtained based on resonance enhanced two photon ionization detection at the parent mass.[16] The spectrum turned out to be complicated with many more bands than expected from normal mode calculations. In this paper we present an analysis of the spectrum based on double resonance spectroscopy according to which the R2PI spectrum consists of overlapping spectra of three different tautomers of guanine. By using chemical substitution and comparison with IR–UV data and *ab initio* calculations we were able to confidently assign the spectra to the 9H-Enol and 9H- and 7H-Keto tautomers of guanine, respectively.

II. EXPERIMENTAL AND THEORETICAL METHODS

The measurements were performed with an apparatus described in detail elsewhere.[17] In short, material is laser desorbed from a graphite sample in front of a pulsed nozzle. Typical fluences of the Nd:YAG desorption laser operated at 1064 nm (where graphite absorbs but guanine does not) are about 1 mJ/cm^2 or less, which is considerably lower than the fluences normally used for ablation. The laser is focused to a spot of about 0.5 mm diameter within 2 mm in front of the nozzle. We used a pulsed valve (General Valve; Iota One) with a nozzle diameter of 1 mm at a backing pressure of about 5 atmospheres argon drive gas. In some experiments we used CO_2 as drive gas to obtain more intense spectra. The ionization lasers cross the skimmed molecular beam at right angles inside the source region of a reflectron time-of-flight (TOF) mass spectrometer. By monitoring the mass peak at $m/e=151$ of guanine while varying the two photon, one color ionization wavelength, we obtain resonant two photon ionization (R2PI) mass selected excitation spectra. We perform spectral hole burning (SHB) by using two counterpropagating dye laser pulses with a delay of about 150 ns. This generates two peaks in the TOF spectrum—the first from the ''burn'' laser and the second from the ''probe'' laser. When both lasers are tuned to a resonance of the same tautomer, the burn laser causes a decrease in the signal of the probe laser. Generally, we scan the burn laser while the probe laser frequency is fixed to an intense band of one tautomer. If a significant band of the R2PI spectrum is missing in the burn spectrum it belongs to another tautomer (or to a hot band, which however we generally do not observe in our guanine spectra). In the next step we probe at this frequency while scanning the pump laser to reveal the spectrum of the next tautomer.

We perform IR–UV SHB with the same method but taking a difference frequency IR laser as the burn laser. The radiation from an infrared dye (a mixture of Styryl 8 and Styryl 9) is aligned collinearly with the perpendicularly polarized ND:YAG fundamental (1064 nm) and directed through a MgO-doped $LiNbO_3$ crystal to generate 3300–

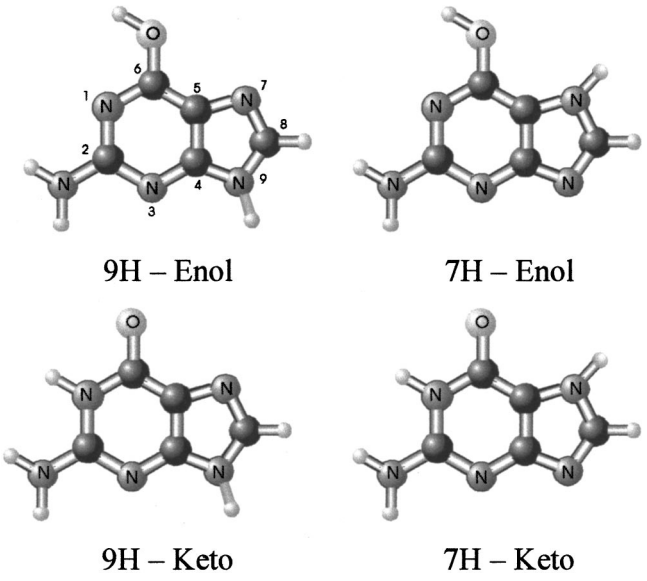

FIG. 1. The Keto-/Enol(*trans*)- and 9H-/7H-tautomers of guanine.

4000 cm^{-1} tunable IR light. Suitable dielectric mirrors separate the ND:YAG fundamental and the dye laser beam behind the crystal. We typically use 50 mJ of the YAG fundamental and 10 mJ of the dye laser to obtain around 1 mJ/pulse IR radiation between 3300 and 4000 cm^{-1} with a bandwidth of <0.1 cm^{-1}. The IR laser is calibrated by recording a water vapor spectrum. Color centers in the $LiNbO_3$ crystal lead to a decrease of the IR intensity from 3515 to 3550 cm^{-1}. In that spectral range we use another $LiNbO_3$ crystal with a gap in another region.

We have carried out calculations using the GAUSSIAN 98 program package.[18] We performed Møller–Plesset second order perturbation theory (MP2) calculations utilizing a 6-311G(d,p) basis set. We have fully optimized all structures on the respective level with 10^{-8} hartree as SCF convergence criterion and 1.5×10^{-5} hartree/bohr and hartree/degree, respectively, as convergence criterion for the gradient optimization of the structures. We obtained the vibrational frequencies by performing a normal mode analysis on the optimized geometries using analytical gradients of the energy. The stabilization energies were corrected for the zero point energy (ZPE) using the harmonic frequencies calculated at the respective level of theory.

III. RESULTS AND DISCUSSION

Figure 1 shows the Keto-/Enol- and 7H-/9H-tautomers of guanine. According to the MP2/6-31G(d,p) calculations of 36 guanine isomers in Ref. 19 the 9H- and the 7H-Keto tautomers are the most stable ones with very similar electronic energies. They are followed by the two 9H-Enol isomers with the OH group pointing to the five ring (*cis* form) and away from it (*trans* form) at 595 cm^{-1} (7.1 kJ/mol) and 385 cm^{-1} (4.7 kJ/mol) higher energy, respectively.[19] The 7H-Enol tautomer is already less stable by more than 16 kJ/mol. These calculations do not include corrections for the vibrational zero point energy. Table I shows the relative stabilization energies of these five tautomers of guanine at the MP2/6-311G(d,p) level after correction for the zero point vibrational energy calculated at this level. The energy sequence did not change, i.e., the 9H- and 7H-Keto and the 9H-(*trans*)Enol tautomers have similar energies while the 7H-Enol tautomer is considerably less stable.

Figure 2 schematically shows the 42 normal mode vibrations of the 9H-Enol tautomer as obtained from the force constant matrix calculated at the *cis*/6-31G(d,p) level of theory based on the fully optimized 9H-Enol geometry. As already obtained from a number of calculations at different levels of theory,[20–23] the pyrimidine ring and the amino nitrogen atom are in the same plane while the hydrogen atoms of the amino group are slightly nonplanar in the electronic ground state. The *cis* calculation leads to a completely planar geometry of the 9H-Enol tautomer in the S_1 state, i.e., the amino group is planar here, too.

The S_0 state normal mode frequencies of the five most stable tautomers of guanine are listed in Table II in order of increasing frequency as calculated at the MP2/6-311G(d,p) level. Additionally the *cis* 6-31G(d,p) frequencies of the S_1 state of *trans*-9H-Enol-guanine are given. Figure 3 shows the R2PI and UV–UV double resonance spectra of guanine, revealing three different tautomers in the investigated wavelength range. There is no decrease of the ion signal by burning at longer wavelengths than 32 870 cm^{-1} for trace *c*, 32 870+405 cm^{-1} for trace *b*, and 32 870+1044 cm^{-1} for trace *a*, which are therefore the electronic origins of three different tautomers.

Figure 4 shows the R2PI and UV–UV double resonance spectra of 1-methylguanine and guanine for comparison. The SHB spectra show that two tautomers of 1-methylguanine exist in the gas phase. Only the Keto tautomer can be formed

TABLE I. Stabilization energies of five tautomers of guanine at the MP2/6-311G(d,p) level corrected for the zero point vibrational energy (kJ/mole).

	9H-Keto	7H-Keto	9H-Enol *trans*	9H-Enol *cis*	7H-Enol *trans*
Electronic energy	−1 421 028	−1 421 027	−1 421 025	−1 421 022	−1 421 010
Zero point energy	308	308	309	309	308
Sum of electronic and zero point energy	−1 420 720	−1 420 719	−1 420 716	−1 420 713	−1 420 702
Relative energy	0	1	4	7	18

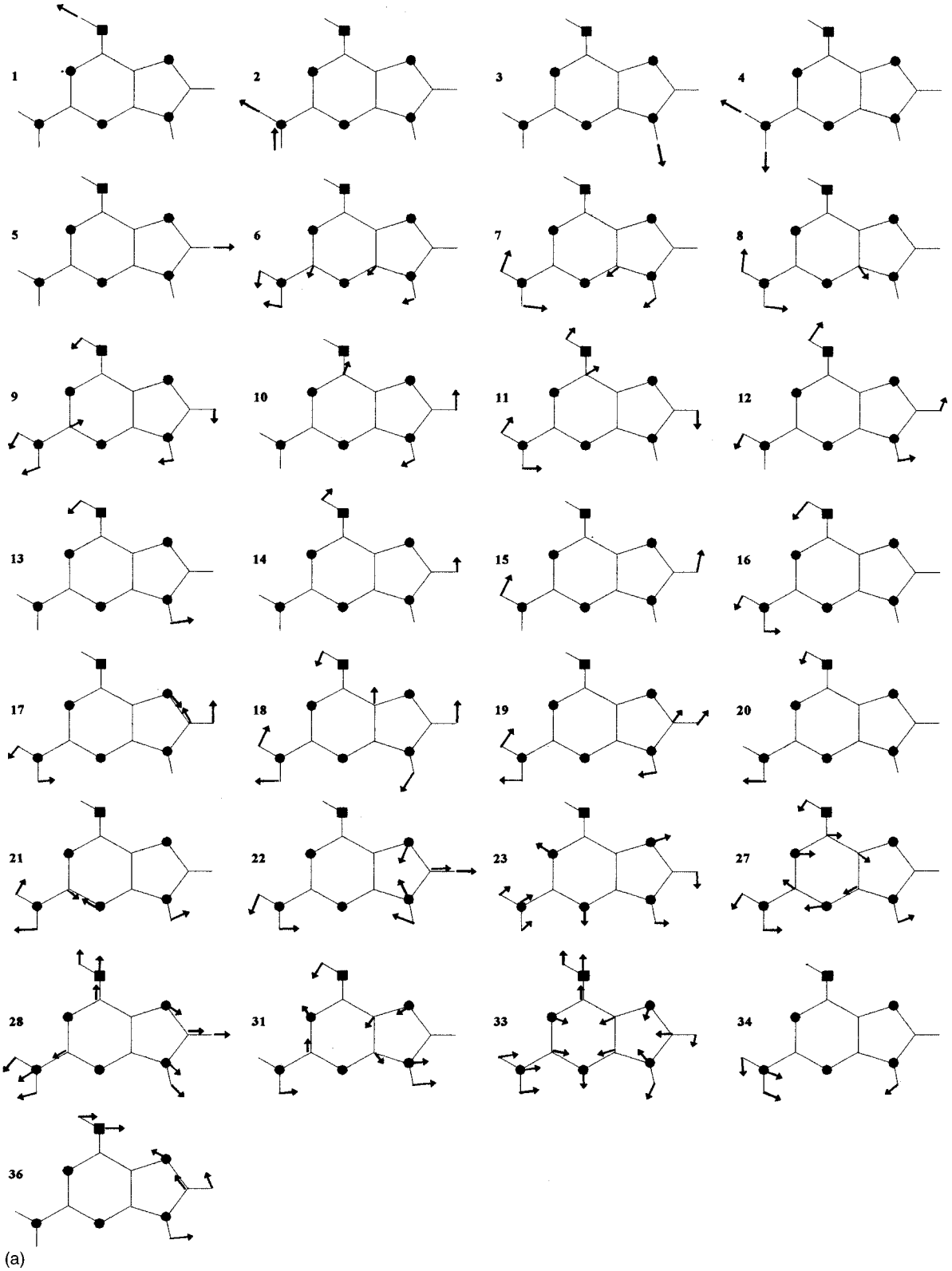

FIG. 2. The S_1 state normal mode vibrations of 9H-Enol guanine(*trans*) obtained from the CIS calculations. (a) In-plane vibrations; (b) out-of-plane vibrations.

here because position N1 of guanine is blocked. Careful line by line inspection of the two SHB spectra *a* and *b* of 1-methylguanine shows that their vibronic patterns are very similar; cf. Fig. 4. This is expected for two Keto tautomers which differ only in the 9H- and 7H-position; cf. Table II. A careful inspection of the guanine spectra in Fig. 4 shows that traces *a* and *b* of guanine resemble quite closely and look different from trace *c*. The SHB spectra of the guanine tau-

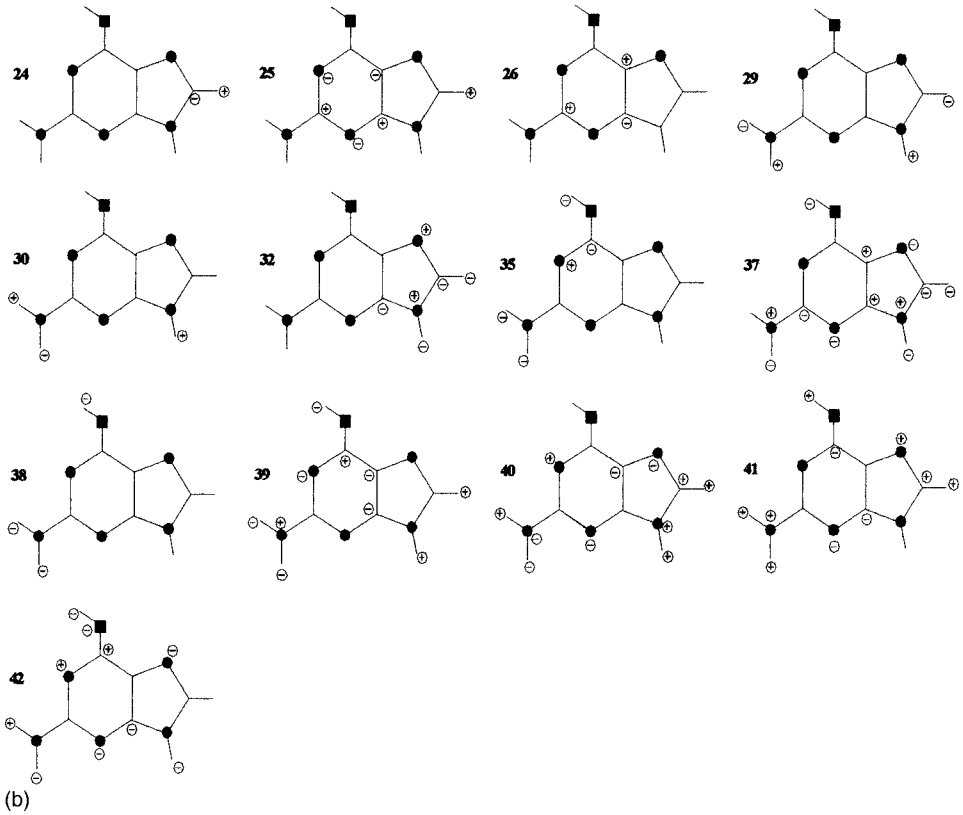

FIG. 2. (*Continued.*)

tomers *a* and *b* but not of tautomer *c* overlap reasonably well with the SHB spectra of 1-methylguanine. This is a first hint to assign guanine tautomer *c* to the Enol form and guanine tautomers *a* and *b* to the Keto form.

The OH- and NH-stretch vibrations are very specific for the Keto or Enol structure but not Franck–Condon active in our vibronic spectra. To obtain isomer selective infrared spectra we have performed IR–UV double resonance experiments. The spectra obtained for tautomer *a*, *b*, and *c* and the two tautomers of 1-methylguanine are displayed in Figs. 5 and 6, respectively. Guanine tautomer *c* shows four IR bands at 3587, 3577, 3516, and 3462 cm^{-1} while tautomers *a* and *b* have their two highest frequencies at 3505/3490 cm^{-1} and 3505/3497 cm^{-1}. The latter frequencies are very similar to those of the two tautomers of 1-methylguanine (Enol form blocked) with highest frequencies of 3505/3489 and 3505/3495 cm^{-1}. This again points strongly to tautomers *a* and *b* as the Keto tautomers. The calculations in Table II indeed show that the NH-stretch vibrations have lower frequencies in the Keto tautomers compared to the Enol tautomers. The highest frequency in the spectrum of tautomer *c* is at 3587 cm^{-1} and can be ascribed to the OH-stretch vibration of the Enol form which of course is missing in the Keto form. The bands at 3577 cm^{-1} in the Enol tautomer and at 3505 cm^{-1} in the Keto tautomers are the antisymmetric NH_2-stretch vibrations with a frequency difference in good agreement with the MP2 calculations. Hence the assignment of tautomer *c* to an Enol form and tautomers *a* and *b* to Keto forms is completely consistent.

Which Keto forms do we observe? The calculations presented in Table I show that the 9H- and 7H-Keto tautomers are the most stable guanine isomers with very similar stabilization energies. We expect both tautomers to be abundant in the jet. The MP2 calculations show a larger frequency difference between mode 1 and 2 (NH_2 antisymmetric stretch and N9H/N7H-stretch vibration) in the 9H-Keto tautomer than in the 7H-Keto tautomer. On that score it seems reasonable to assign the guanine tautomers *a* and *b* and the 1-methylguanine tautomers *a* and *b* to the 7H- and 9H-tautomers, respectively; cf. Fig. 6. On the other hand, Table II shows that the N9–H frequency is calculated to be larger than the N7–H frequency which leads to the reverse assignment. Therefore we cannot safely assign the two keto spectra to either of the two forms. The N1–H stretch vibrations of the Keto tautomers (cf. Fig. 1) at 3456 cm^{-1} and 3450 cm^{-1} are missing in the 1-methylguanine spectra confirming their assignment. The symmetric NH_2-stretch vibrations show a quite prominent absorption at 3462 cm^{-1} in the Enol tautomer but absorb only weakly in the Keto tautomers (3420 cm^{-1} in the 9H tautomer of 1-methylguanine). Figure 5 and Table III show that the agreement of the experimental and calculated infrared frequencies is generally very good.

Which Enol form do we observe? The MP2 calculations in Table I show that the 9H-Enol tautomer is considerably more stable than the 7H-Enol tautomer (14 kJ/mol stabilization energy difference) while the 9H-/7H-Keto tautomers have very similar energies. Hence it is reasonable to expect that only the 9H-Enol tautomer is abundant in the jet con-

TABLE II. The normal mode frequencies of five tautomers of guanine calculated at the MP2/6-311G(d,p) level and of trans 9H-Enol guanine on the CIS 6-31G(d,p) level (rightmost column). In this column the vibrations of 9H-Enol guanine are assigned according to the modes depicted in Fig. 2. The frequencies of the other tautomers are set in order according to size (cm^{-1}).

	S_0 state MP2 6-311G(d,p)					S_1 state CIS 6-31G(d,p)
	9H			7H		9H
Mode	*trans*-Enol	CIS-Enol	Keto	Keto	Enol	*trans*-Enol
42	131	134	130	140	134	64
41	182	177	154	148	170	102
40	244	243	194	183	243	215
39	300	283	313	300	290	249
38	336	340	331	324	334	267
37	346	347	333	333	355	275
36	438	455	360	369	426	311
35	498	490	487	487	433	359
34	504	508	522	501	466	365
33	516	511	527	537	503	492
32	546	546	576	569	554	521
31	591	578	619	623	608	554
30	634	633	629	631	632	625
29	655	646	661	661	636	634
28	660	654	665	672	660	653
27	661	678	683	701	661	697
26	705	706	732	712	702	722
25	751	751	757	790	753	766
24	822	816	803	815	839	805
23	840	840	838	837	839	878
22	937	939	941	956	951	985
21	1037	1039	1057	1045	1030	1036
20	1096	1100	1091	1091	1081	1101
19	1114	1118	1104	1127	1126	1142
18	1176	1176	1169	1171	1172	1204
17	1237	1245	1185	1219	1232	1250
16	1300	1315	1305	1308	1283	1302
15	1342	1339	1340	1330	1361	1398
14	1408	1408	1394	1403	1401	1451
13	1422	1423	1414	1412	1413	1471
12	1467	1454	1474	1493	1452	1528
11	1482	1488	1507	1503	1499	1562
10	1516	1518	1568	1569	1529	1595
9	1545	1558	1620	1591	1540	1635
8	1646	1644	1635	1635	1639	1715
7	1664	1663	1691	1698	1646	1799
6	1709	1709	1842	1831	1734	1808
5	3281	3283	3286	3287	3279	3445
4	3619	3622	3593	3581	3614	3856
3	3685	3683	3622	3624	3690	3913
2	3746	3751	3680	3677	3740	4006
1	3813	3820	3705	3690	3817	4153

trary to the Keto tautomers where both are observed. The *cis* form of the 9H-Enol tautomer is 3 kJ/mol less stable than the *trans* form. This energy difference is not very large and we cannot exclude that there are minor bands especially in crowded regions of the R2PI spectrum which originate from this isomer. From the comparison of our UV–UV hole burning spectra and the R2PI spectrum we have no evidence of additional bands however.

Based on these tautomer assignments we are able to perform a partial assignment of the in-plane vibrations in the

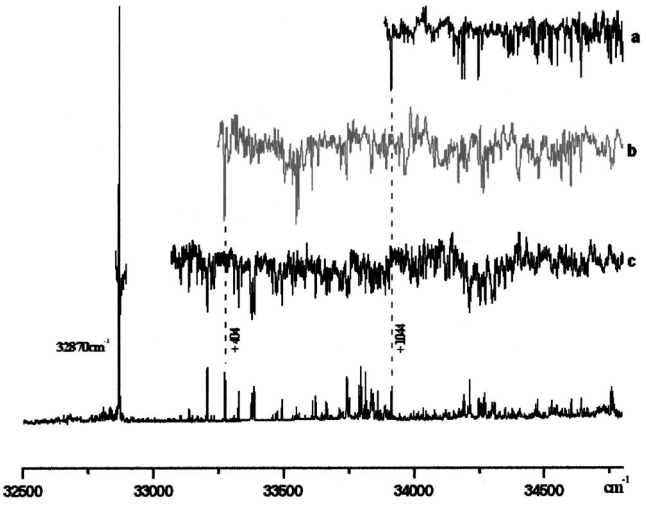

FIG. 3. R2PI and UV–UV double resonance spectra of guanine revealing three different tautomers in the investigated wavelength range. The R2PI spectrum is displayed in the lower trace. The upper traces show the decrease of the ion intensity induced by the probe laser when the pump laser is scanned (SHB spectra).

electronic spectra of the guanine tautomers. Mode 36 and 34 are in-plane ''gearing'' motions of the two rings of guanine accompanied by in-plane C–OH (C═O for the Keto tautomer) and C–N(amino) bending motions, respectively; cf. Fig. 2(a). We assign the intense transition at $0+337\,cm^{-1}$ (336, 333 cm^{-1} for the Keto tautomers) to the excitation of an in-plane gearing motion in the S_1 state accompanied by an C–N(amino) bending motion; cf. Table IV. The R2PI spectra of guanine deuterated at one and at all four acidic positions displayed in Figs. 7(b) and 7(c) support this assignment. Figure 7(b) exhibits the four electronic origins with D substituted in the NHH, NH, and OH positions, respectively, which lie near to the electronic origin of undeuterated guanine dis-

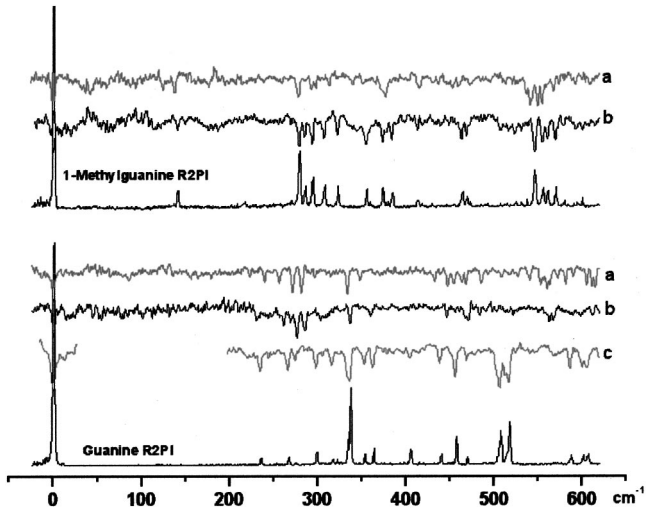

FIG. 4. R2PI and UV–UV double resonance spectra of guanine and 1-methylguanine. For comparison of the vibronic structures the spectra are shifted so that their electronic origin bands overlap. From bottom to top: R2PI spectrum of guanine, SHB spectra of the three tautomers *a, b, c* of guanine, R2PI spectrum of 1-methylguanine, SHB spectra of the two tautomers *a, b* of 1-methylguanine.

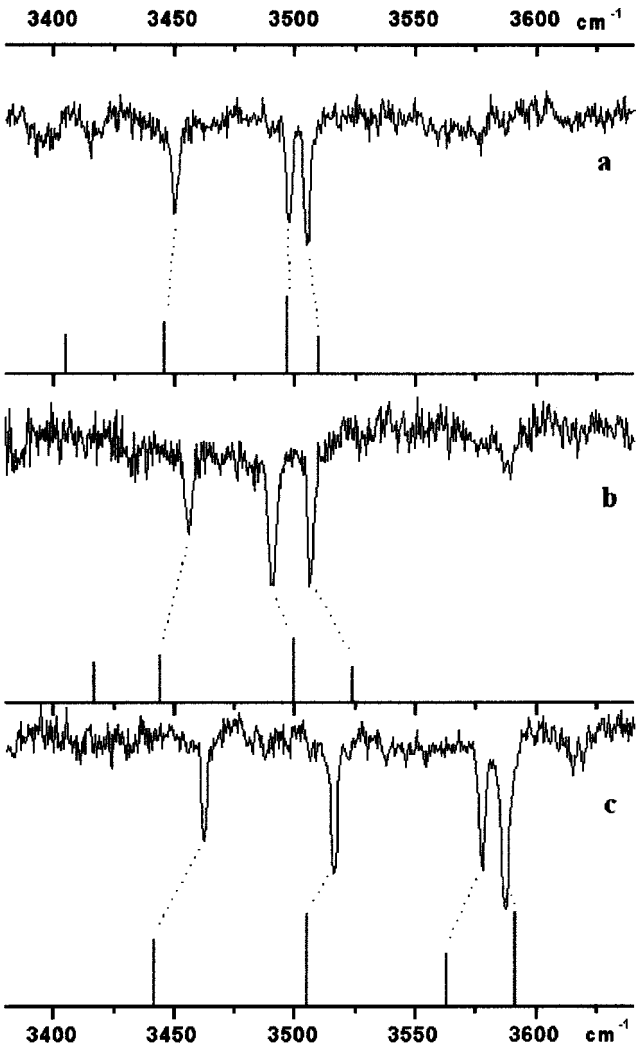

FIG. 5. IR–UV double resonance spectra of (a) guanine tautomer analyzed at 32 870+1044 cm^{-1} (7H-Keto), (b) guanine tautomer analyzed at 32 870 +405 cm^{-1} (9H-Keto), (c) guanine tautomer analyzed at 32 870 cm^{-1} (9H-Enol *trans*) The vibrational frequencies calculated at the MP2 level are shown for comparison. The calculated frequencies are scaled with a factor 0.942 for OH-stretching and 0.951 for NH-stretching vibrations obtained from a comparison of the experimental para-aminophenol IR spectrum with the spectrum calculated at the MP2/6-31G(d,p) level.

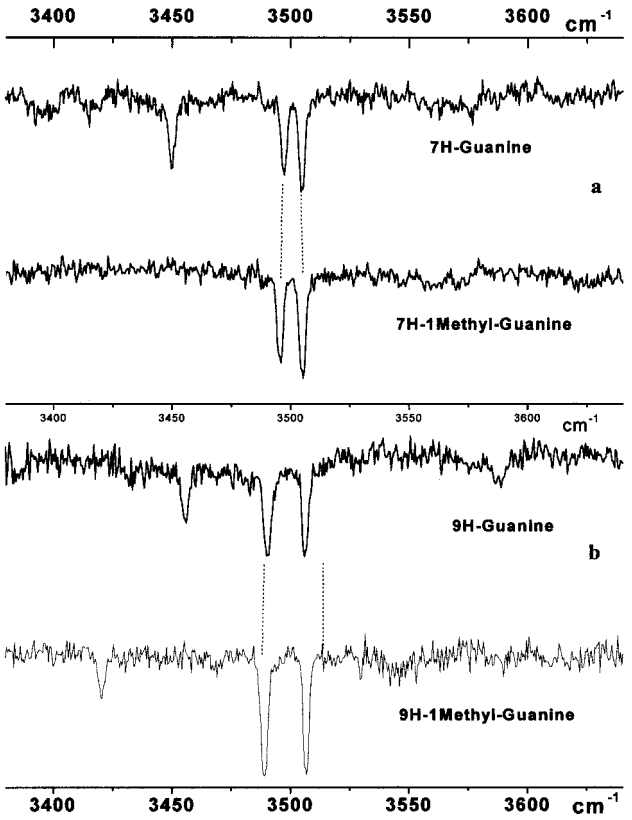

FIG. 6. IR–UV double resonance spectra of (a) 1-methylguanine tautomer analyzed at 32 941 cm^{-1} (7H-Keto), (b) 1-methylguanine tautomer analyzed at 32 941+687 cm^{-1} (9H-Keto). The IR spectra of 9H-/7H-Keto guanine are shown for comparison.

played in Fig. 7(a). The four intense bands around 33 200 cm^{-1} in Fig. 7(b) correspond to the intense band at 0 +337 cm^{-1} in Fig. 7(a). The bands are shifted by 0, 0, −24, and −18 cm^{-1}, respectively, relative to the spectrum of undeuterated guanine if the electronic origins are superimposed. This agrees nicely with the calculated deuteration shifts for mode 34 of the 9H-Enol tautomer in the S_1 state (−2, −3, −20, and −20 cm^{-1} for the OD, N9D, NHD, and NDH isotopomers, respectively) supporting the assignment of this vibration. Mode 36 with a strong C–OH bending component shows a shift of −12 cm^{-1} for the OD isotopomer and nearly zero shift for the N9D, NHD, and NDH isotopomers and can thus be excluded. The d_4-isotopomer in Fig. 7(c) exhibits an intense band at −40 cm^{-1} deuteration shift which can be assigned to mode 34 with a calculated shift of −40 cm^{-1}.

TABLE III. Vibrational assignments of the ground state fundamentals of the different tautomers of guanine and 1-methylguanine in the range of the OH- and NH-stretching vibrations. All values are in cm^{-1}. Calculated frequencies are scaled with 0.942 for OH-stretching and 0.951 for NH-stretching vibrations. All values are in cm^{-1}.

9H-Enol guanine		9H-Keto guanine		7H-Keto guanine		9H-1-methyl-guanine		7H-1-methyl-guanine		Assignment
Expt.	Calc.	Expt.	Calc.	Expt.	Calc.	Expt.	Calc.	Expt.	Calc.	
3587	3591									υOH
3577	3562	3506	3523	3505	3509	3506		3505	3509	$\upsilon NH_2 a$
3516	3504	3490	3499	3497	3496	3489		3496	3497	υN(9/7)H
		3456	3444	3450	3446					υN(1)H
3462	3441		3416		3405	3420			3404	$\upsilon NH_2 s$

TABLE IV. Vibrational assignments of some excited (S_1) state in-plane vibrations of the different tautomers of guanine. All values are in cm^{-1}.

Tautomer *c* (32 878 cm^{-1})	Assignment	Tautomer *b* (+405 cm^{-1})	Tautomer *a* (+1044 cm^{-1})
+337 s	34	336	333
457 s	33	467/470	448
508 s	31		
517 s			
624 m	28		

Mode 33 is essentially a 6-ring stretching motion similar to the vibration 6*a* in substituted benzene rings. For comparison: its frequency is 436/509 cm^{-1} in the S_1 state of *p*-aminophenol (Ref. 24)/benzotriazole (Ref. 25). We assign the rather intense band at 457 cm^{-1} to mode 34 but the bands at 508 or 517 cm^{-1} can be assigned to this motion as well. Mode 31 is an in-plane zig–zag deformation vibration of the two rings; cf. Fig. 2(a). The next in-plane vibration is mode 28 which resembles the ring breathing mode 1 in substituted benzenes. A tentative assignment of the in-plane modes 33, 31, and 28 is given in Table IV.

IV. CONCLUSIONS

We have presented results from UV–UV and IR–UV double resonance experiments on guanine and 1-methyl guanine to assign the R2PI spectrum of guanine to different tautomers. First results on IR–UV experiments are discussed which help to decide between the different tautomers. The vibronic spectrum built on the redmost guanine band at 32 870 cm^{-1} (electronic origin 0) can be traced back to the 9H-Enol tautomer; the spectra built on the origins at $0 + 405\,cm^{-1}$ and $0 + 1044\,cm^{-1}$ stem from the Keto tautomers. The corresponding Keto tautomers of 1-methylguanine have their electronic origins at 32 941 cm^{-1} and 33 628 cm^{-1}. The comparison with the IR and UV spectra of guanine derivatives modified to block the Keto–Enol tautomerism serves as a powerful additional tool for tautomer assignment.

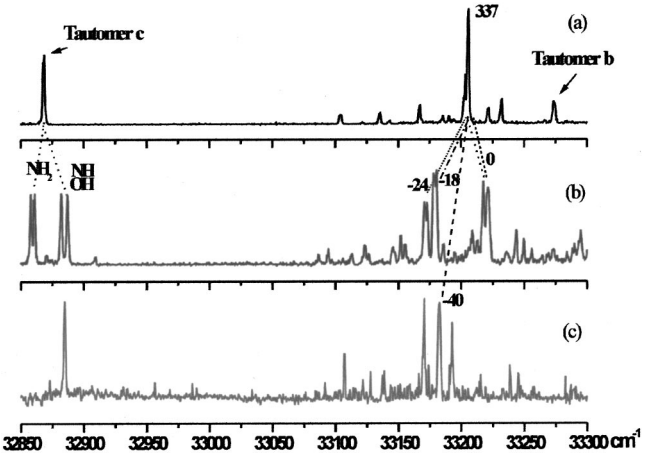

FIG. 7. The R2PI spectra of deuterated guanine (a) *h*5-guanine, (b) *d*1-guanine, (c) *d*4-guanine.

Further experiments can now elucidate the intrinsic properties of the different tautomers of guanine based on this assignment. Information about their precise ionization energies can be obtained by two-color ionization and possibly MATI spectroscopy. The S_0 vibrational frequencies can be measured by ion dip and possibly dispersed fluorescence spectroscopy as well as by further IR–UV experiments. Dispersed fluorescence of selected vibronic transitions would also allow further assignment of the S_1 state vibrations. The weak low frequency vibrations below 300 cm^{-1} above the Enol origin still have to be assigned. Clusters of guanine with cytosine and with itself[26] have to be assigned to specific structures based on extensive double resonance and chemical blocking experiments.[27] These experiments will help to distinguish properties of guanine due to the molecular structure itself from those externally imposed.

ACKNOWLEDGMENTS

This work has been supported by the Deutsche Forschungsgemeinschaft and the United States–Israel Binational Science Foundation.

[1] I. K. Yanson, A. B. Teplitsky, and L. F. Sukhodub, Biopolymers **18**, 1149 (1997).
[2] S. P. Fodor, R. P. Rava, R. A. Copeland, and T. G. Spiro, J. Raman Spectrosc. **17**, 471 (1986).
[3] H. Urabe, H. Hayashi, Y. Tominaga, Y. Nishimura, K. Kubota, and M. Zsuboi, J. Chem. Phys. **82**, 531 (1985).
[4] S. Cocco and R. Monasson, J. Chem. Phys. **112**, 10017 (2000).
[5] B. B. Brady, L. A. Peteanu, and D. H. Levy, Chem. Phys. Lett. **147**, 538 (1988).
[6] M. R. Viant, R. S. Fellers, R. P. Mc Laughlin, and R. J. Saykally, J. Chem. Phys. **103**, 9502 (1995).
[7] R. D. Brown, P. D. Godfrey, D. McNaughton, and A. P. Pierlot, J. Chem. Soc. Chem. Commun. **1**, 37 (1989).
[8] K. Liu, R. S. Fellers, M. R. Viant, R. P. McLaughlin, Mac G. Brown, and R. J. Saykally, Rev. Sci. Instrum. **67**, 410 (1996).
[9] M. R. Viant, R. S. Fellers, R. P. McLaughlin, and R. J. Saykally, J. Chem. Phys. **103**, 9502 (1995).
[10] P. Colarusso, K. Zhang, B. Guo, and P. F. Bernath, Chem. Phys. Lett. **269**, 39 (1997).
[11] R. D. Brown, P. D. Godfrey, D. McNaughton, and A. P. Pierlot, J. Am. Chem. Soc. **110**, 2329 (1988).
[12] W. Caminati, G. Maccaferri, P. G. Favero, and L. B. Favero, Chem. Phys. Lett. **251**, 189 (1996).
[13] S. Keun Kim, W. Lee, and D. R. Herschbach, J. Phys. Chem. **100**, 7933 (1996).
[14] R. D. Brown, P. D. Godfrey, D. McNaughton, and A. P. Pierlot, J. Am. Chem. Soc. **110**, 2308 (1989).
[15] B. B. Brady, L. A. Peteanu, and D. H. Levy, Chem. Phys. Lett. **147**, 538 (1988).
[16] E. Nir, L. Grace, B. Brauer, and M. S. de Vries, J. Am. Chem. Soc. **121**, 4896 (1999).
[17] G. Meijer, M. S. de Vries, H. E. Hunzicker, and H. R. Wendt, Appl. Phys. B: Photophys. Laser Chem. **51**, 395 (1990).
[18] M. J. Frisch, G. W. Trucks, H. B. Schlegel *et al.*, GAUSSIAN 98, Revision A.4, Gaussian, Inc., Pittsburgh, 1995.
[19] T. Ha, H.-J. Keller, R. Gunde, and H.-H. Gunthard, J. Phys. Chem. A **103**, 6612 (1999).
[20] R. Santamaria, E. Charro, A. Zacarias, and M. Castro, J. Comput. Chem. **20**, 511 (1999).
[21] J. Sponer, J. Leszczynski, and P. Hobza, J. Phys. Chem. **100**, 1965 (1995).
[22] P. Hobza, M. Kabelac, J. Sponer, P. Mejzlik, and J. Vondrasek, J. Comput. Chem. **18**, 1136 (1997).
[23] P. Hobza and J. Sponer, Chem. Phys. Lett. **261**, 379 (1996).

[24] S. Wategaonkar and S. Doraiswamy, J. Chem. Phys. **105**, 1786 (1996).
[25] W. Roth, C. Jacoby, A. Westphal, and M. Schmitt, J. Phys. Chem. A **102**, 3048 (1998); C. Jacoby, P. Hering, M. Schmitt, W. Roth, and K. Kleinermanns, Chem. Phys. **239**, 23 (1998).
[26] E. Nir, K. Kleinermanns, and M. S. de Vries, Nature (London) **408**, 949 (2000).
[27] E. Nir, Ch. Janzen, P. Imhof, K. Kleinermanns, and M. S. de Vries (unpublished).